4350 *Chem. Mater.* **2010,** *22,* 4350–4352
DOI:10.1021/cm100962t

CHEMISTRY OF MATERIALS
Communication

Uniform Decoration of Linker-Free Quantum Dots onto Mesoporous TiO_2 Using Liquid Carbon Dioxide

Wonho Jang,[†,‡] Daejin Kim,[†] Jaehoon Kim,*[,†] Byoung Koun Min,*[,†] Jae-Duck Kim,[†] and Ki-pung Yoo[‡]

[†]*Clean Energy Center, Energy Division, Korea Institute of Science and Technology (KIST), 39-1 Hawolgok-dong, Seongbuk-gu, Seoul, 131-791, Korea, and* [‡]*Department of Chemical and Biomolecular Engineering, Sogang University, 1 Shinsu-dong, Mapo-gu, Seoul 121-742, Korea*

Received April 7, 2010
Revised Manuscript Received July 7, 2010

Following the pioneering works of mesoporous TiO_2 based dye-sensitized solar cell (DSSC) by Grätzel and coworkers, this solar cell architecture has received considerable attention as a low cost alternative to conventional silicon-based solar cells.[1] Quantum dot (QD) sensitized solar cells (QDSSCs) are also a type of DSSC architecture in which inorganic semiconductor QDs such as CdS, PbS, CdSe, and InP absorb light and photoexcited electrons are transferred to the TiO_2 electrode. Because of the beneficial properties of QDs including high extinction coefficients, tunable band gap, resistance to photobleaching, and higher stability over organic dyes, QDSSCs have been expected to be superior to DSSCs.[2] Moreover, the demonstration of multiple exciton generation by impact ionization associated with QDs has provided the possibility of solar cell efficiency over the thermodynamic limit of silicon-based solar cells (32%).[2b,3] In spite of the advantages, the current status of QDSSCs is much below the expectations because various obstacles have unraveled such as inappropriate redox couples, inefficient electron transfer at the interface, and charge recombination.[4] In addition, poor deposition of QDs onto the mesoporous TiO_2 film has been addressed as a major huddle for high energy conversion efficiency.[2b,c,4] To maximize the light absorption and facilitate electron transfer, QDs need to strongly anchor and decorate uniformly throughout the TiO_2 electrode.[4]

Typical TiO_2 electrodes are prepared by sintering TiO_2 nanoparticles and forming meso- or nanoporous films a few micrometers thick. In order to decorate a whole TiO_2 film with QDs, QDs or precursor ions should penetrate throughout the mesoporous TiO_2 film. To date, several methods have been employed for depositing QDs onto TiO_2 films such as the self-assembled monolayer (SAM), chemical bath deposition (CBD), and successive ionic layer adsorption and reaction (SILAR) methods.[2c] In the SAM method, presynthesized colloidal QDs dispersed in organic solvents are deposited on the surface of the oxide electrode using bifunctional organic linkers. In the CBD and SILAR methods, QDs are directly grown on the oxide electrode by dipping the oxide layer into aqueous solutions of precursors (e.g., $Cd(NO_3)_2$ and Na_2S for CdS). In the precursor, ions (e.g., Cd^{2+} and S^{2-} ions) penetrate into the mesoporous oxide film, and QDs are deposited onto the oxide film via the chemical reaction between the positive and the negative ionic species. The CBD and SILAR methods have been proven to be more promising techniques to fabricate QDSSC compared to the SAM method.[2c]

A typical solvent used in the CBD or SILAR method, such as water, has a high surface tension and a high viscosity (water surface tension, 73.5 mJ/m^2; water viscosity, 1.14 cP at 15 °C). This makes it difficult for the precursor ions to reach deep inside of the oxide film, often resulting in poor surface decoration of QDs inside the film. For example, when water-based CBD was used, the concentration of CdS in the mesoporous TiO_2 film substantially decreased with respect to the depth of the film.[5] When ethanol was used as a low surface tension (22.8 mJ/m^2 at 15 °C) solvent in the CBD or SILAR method, better penetration of QD precursors into the mesoporous TiO_2 film and more homogeneous QD deposition along the oxide layer were observed.[6] Moreover, better light absorbance and higher energy conversion efficiency were also obtained compared to those of the water-based counterpart.

In this Communication, we describe the first use of liquid carbon dioxide (*l*-CO_2) for uniform deposition of QDs (CdS, PbS and CuS) 2−5 nm in diameter throughout a mesoporous TiO_2 film using the SILAR method. The extremely low viscosity of *l*-CO_2 (1.95 mJ/m^2 at 15 °C) makes it an excellent wetting agent and facilitates the penetration of CO_2-soluble QD precursors into small pores. In addition, the extremely low surface tension of *l*-CO_2 (0.074 cP at 15 °C) leads to faster diffusion of the CO_2-soluble precursors into the mesoporous oxide film and therefore helps alleviate solute concentration gradients. Low surface tension combined with higher solute diffusion rates make *l*-CO_2 particularly suitable for the deposition of QDs onto highly porous and/or nanostructured surfaces. The unique physical properties of supercritical carbon dioxide or *l*-CO_2, including extremely low surface tension, low viscosity, and tunable density, have been

(1) O'regan, B.; Grätzel, M. *Nature* **1991**, *353*, 737–740.
(2) (a) Kamat, P. V. *J. Phys. Chem. C* **2008**, *112*, 18737–18753. (b) Klimov, V. I. *J. Phys. Chem. B* **2006**, *110*, 16827–16845. (c) Mora-Seró, I.; Giménez, S.; Fabregat-Santiago, F.; Gómez, R.; Shen, Q.; Toyoda, T.; Bisquert, J. *Acc. Chem. Res.* **2009**, *42*, 1848–1857.
(3) Nozik, A. J. *Phys. E* **2002**, *14*, 115–200.
(4) Hodes, G. *J. Phys. Chem. C* **2008**, *112*, 17778–17787.
(5) Shalom, M.; Dor, S.; Rühle, S.; Grinis, L.; Zaban, A. *J. Phys. Chem. C* **2009**, *113*, 3895–3898.
(6) (a) Chang, C. H.; Lee, Y. L. *Appl. Phys. Lett.* **2007**, *91*, 053503/1–053503/3. (b) Lee, H.; Wang, M.; Chen, P.; Gamelin, D. R.; Zakeeruddin, S. M.; Grätzel, M.; Nazeeruddin, M. K. *Nano Lett.* **2009**, *9*, 4221–4227.

 Published on Web 07/13/2010

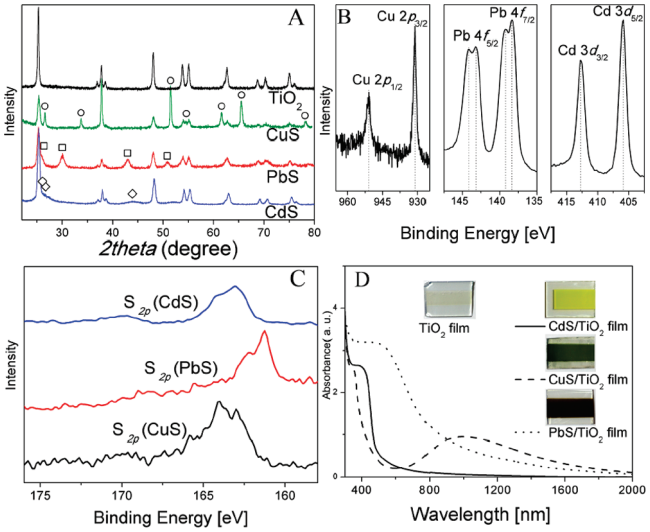

Figure 1. (a) Wide angle X-ray diffraction patterns, (b) high-resolution XPS spectra of Cd, Cu, and Pb, (c) high-resolution XPS spectra of S, and (d) UV−vis absorption spectra of the QDs deposited onto the mesoporous TiO_2 film on glass. $Cu(hfac)_2 \cdot H_2O$, $Pb(hfac)_2$,and $Cd(hfac)_2$ concentrations were 3.0, 0.2, 0.4 wt %, respectively. The QDs on TiO_2 were prepared at the first cycle of deposition.The absoption spectra of QD/TiO_2 were presented by substrating the plain TiO_2 absorption spectrum.

utilized in metal nanoparticle deposition as well as organic or metallic film deposition to enhance gap filling in very high-aspect-ratio structures.[7] For example, highly dispersed and nanosized metal particles (Pt, Pd, Ru, and Rh with a diameter of 1−5 nm) has been deposited on high-surface-area supports using $scCO_2$ or l-CO_2 .[7a,d,e] In addition, copper film on a high-aspect-ratio structure with complete gap-filling was deposited using $scCO_2$ for next generation interconnect applications in microelectronics.[7b] Herein, we first demonstrated the uniform deposition of metal sulfide QDs on the mesoporous oxide film.

To deposit QDs onto the mesoporous TiO_2 layer, metal hexafluoroacetylacetonate species (e.g., $Cu(hfac)_2$, $Pb(hfac)_2$, or $Cd(hfac)_2$) in l-CO_2 were absorbed on the TiO_2 layer followed by reacting the absorbed precursors with a gas phase H_2S, as described in the following equation;

$$M(hfac)_2 + H_2S \rightarrow 2H(hfac) + MS$$

where M indicates Cu, Pb, or Cd. The formation of the metal sulfides from contacting the metal hexafluoroacetylacetonate species and H_2S was found to be very reactive; therefore, the whole deposition process of CuS, PbS or CdS QDs onto the TiO_2 film was carried out at a low temperature (15 °C). Details of the coating apparatus and procedure are described in Supporting Information (see Figure S1).

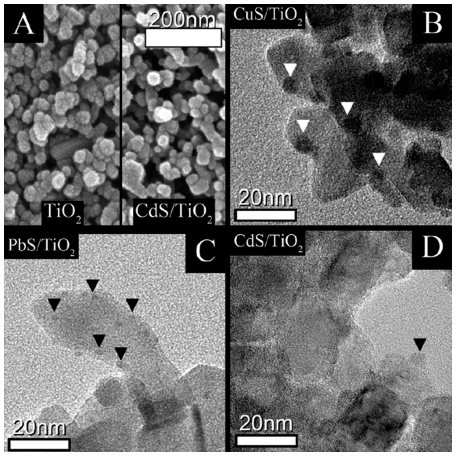

Figure 2. (a) SEM images of the bare TiO_2 film and CdS deposited on TiO_2 film. HR-TEM images of (b) CuS, (c) PbS, and (d) CdS deposited on the mesoporous TiO_2 film. $Cu(hfac)_2 \cdot H_2O$, $Pb(hfac)_2$, and $Cd(hfac)_2$ concentrations were 3.0, 0.2, 0.4 wt %, respectively. The QDs on TiO_2 were prepared at the first cycle of deposition.(▼: QDs).

The structural and compositional characteristics of the QDs deposited on mesoporous TiO_2 film were investigated using wide-angle X-ray diffractometry (XRD) and X-ray photoelectron spectroscopy (XPS), as shown in Figures 1a−c. The XRD spectra of the QD deposited TiO_2 films showed both TiO_2 and metal sulfide peaks. The metal sulfide peaks are well matched with the XRD database of CuS (JCPDS 06-0464), PbS (JCPDS 05-0592), and CdS (JCPDS 75-0581), indicating the formation of stoichiometric metal sulfide QDs. The formation of stoichiometric metal sulfide was also confirmed by XPS. As shown in Figures 1b and c, the XPS peaks of S (2p at 164.0 eV for CuS, at 161.2 eV for PbS and at 163.1 eV for CdS), Cu ($2p_{1/2}$ at 951.1 eV and $2p_{3/2}$ at 931.1 eV), Pb ($4f_{5/2}$ at 143.1 and 144.2 eV; $4f_{7/2}$ at 138.1 and 139.3 eV), and Cd ($3d_{3/2}$ at 413.1 eV ; $3d_{5/2}$ at 406.4 eV) are in agreement with the previously reported binding energies.[8] Atomic composition analysis also further confirmed the 1:1 molar ratios of Cu:S, Pb:S, and Cd:S.

The optical characteristics of QDs on the mesoporous TiO_2 were also investigated by UV−vis spectroscopy. As shown in Figure 1d, the absorption band edge of PbS/TiO_2 and CdS/TiO_2 are in the visible region. The excitonic peaks of PbS at ~406 nm and of CdS at ~378 nm indicate that the size of QDs are very small. By comparing these data with the previously reported values, the size of PbS and CdS was estimated to be less than 5 nm.[9] The absorption edge of CuS at ~500 nm showed a huge blue shift compared to that of the CuS nanodisks with a size of 20 nm (620 nm), indicating the formation of nanosized CuS crystallites.[10] Overall, the XRD, XPS, and UV−vis absorption data clearly suggest that the stoichiometric

(7) (a) Morley, K. S.; Marr, P. C.; Webb, P. B.; Berry, A. R.; Allison, F. J.; Moldovan, G.; Brownb, P. D.; Howdle, S. M. *J. Mater. Chem.* **2002**, *12*, 1898–1905. (b) Blackburn, J. M.; Long, D. P.; Cabañas, A.; Watkins, J. J. *Science* **2001**, *294*, 141–145. (c) Hunde, E. T.; Watkins, J. J. *Chem. Mater.* **2004**, *16*, 498–503. (d) Saquing, C. D.; Kang, D.; Aindow, M.; Erkey, C. *Microporous Mesoporous Mater.* **2005**, *80*, 11–23. (e) Kim, J.; Roberts, G. W.; Kiserow, D. J. *Chem. Mater.* **2006**, *18*, 4710–4712. (f) O'Neil, A.; Watkins, J. J. *Chem. Mater.* **2006**, *18*, 5652–5658. (g) Smetana, A. B.; Wang, J. S.; Boeckl, J. J.; Brown, G. J.; Wai, C. M. *J. Phys. Chem. C* **2008**, *112*, 2294–2297.

(8) (a) Leloup, J.; Ruaudel-Teixier, A.; Barraud, A.; Roulet, H.; Dufour, G. *Appl. Surf. Sci.* **1993**, *68*, 231–242. (b) Reichea, R.; Thielschb, R.; Oswalda, S.; Wetziga, K. *J. Electron Spectrosc. Relat. Phenom.* **1999**, *104*, 161–171. (c) Mondal, S. P.; Dhar, A.; Ray, S. K.; Chakraborty, A. K. *J. Appl. Phys.* **2009**, *105*, 084309/1–084309/5.

(9) (a) Yu, W. W.; Qu, L.; Guo, W.; Peng, Z. *Chem. Mater.* **2003**, *15*, 2854–2860. (b) Moreels, I.; Lambert, K.; Smeets, D.; Muynck, D. D.; Nollet, T.; Martins, J. C.; Vanhaecke, F.; Vantomme, A.; Delerue, C.; Allan, G.; Hens, Z. *ACS Nano* **2009**, *3*, 3023–3030.

(10) Zhang, P.; Gao, L. *J. Mater. Chem.* **2003**, *13*, 2007–2010.

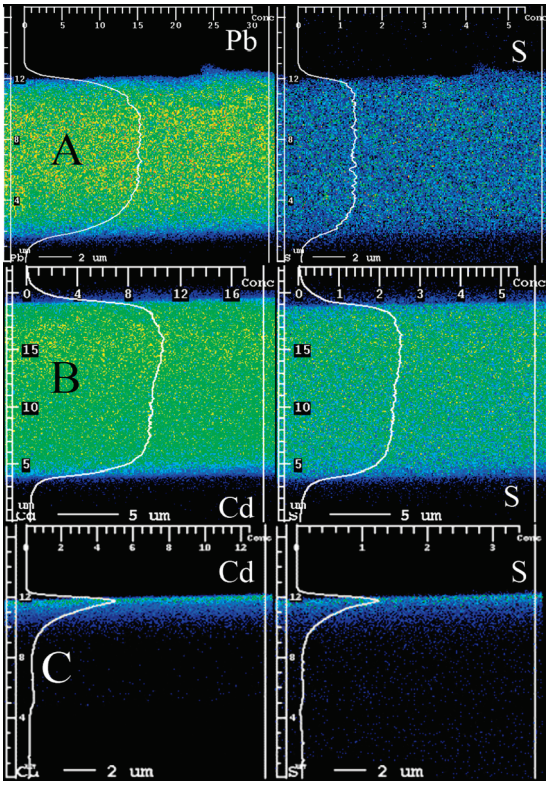

Figure 3. EPMA depth profiles of (a) PbS and (b) CdS QDs deposited onto the mesoporous TiO_2 film using *l*-CO_2. (c) EPMA depth profiles of CdS QDs deposited onto the mesoporous TiO_2 film using acetone. $Cu(hfac)_2 \cdot H_2O$, $Pb(hfac)_2$, and $Cd(hfac)_2$ concentrations were 3.0, 0.2, 0.4 wt %, respectively. The *x*-axis is weight percent. Higher metal concentration compared to that of sulfur due to the EPMA depth profile is expressed as weight percent.

metal chalcogenide QDs were successively synthesized on the mesoporous TiO_2 film using the *l*-CO_2 coating and subsequent reaction technique.

The morphologies of the QDs deposited on the mesoporous TiO_2 were investigated by high-resolution transmission electron microscopy (HR-TEM) and scanning elelctron microscopy (SEM), as shown in Figure 2. Since the SEM images did not reveal QDs, the apparent difference between the bare TiO_2 film and QD deposited TiO_2 film was not observed as seen in Figure 2a. Closer inspection by HR-TEM showed that well-separated and single-crystalline QDs were deposited on the TiO_2 surface. The average size of CuS, PbS, and CdS QDs was estimated to be ~5, ~4, and ~2 nm, respectively. It is noteworthy that the size of QDs is easily controllable by adjusting the precursor concentration (see Figure S2 in the Supporting Information).

To check the uniformity of the QDs throughout the TiO_2 film (~15 μm thick), a depth profile of the PbS or CdS deposited TiO_2 films was measured by electron probe microanalysis (EPMA) and a XPS depth profiling (Figure 3). The concentration of Pb, Cd, or S throughout the TiO_2 film was very uniform from the surface to the bottom of the film (Figures 3a−b). In addition, the concentration of QDs near the top surface of the film (~ 1 μm) was also very uniform (see Figure S3 in Supporting Information). For comparison, CdS was also deposited on TiO_2 using acetone (surface tension, 24.0 mJ/m^2 at 15 °C; viscosity, 0.34 cP) as a model solvent under coating conditions identical to those of *l*-CO_2. Both Cd and S were detected in only the narrow region near the surface, particularly concentrated in the first tenth of the TiO_2 layers (~1.5 μm). This clearly indicates that the low surface tension and viscosity of the solvent is critical for uniform decoration of QDs onto the mesoporous TiO_2 film. Furthermore, the low surface tension leads to low capillary force in the pores during drying, which results in homogeneous deposition of the precursor without severe aggregation.

Finally, we tested the feasibility of the CdS and PbS QDs deposited on the TiO_2 electrode using *l*-CO_2 in the QDSSC application. The polysulfide electrolyte[11] (for CdS) or iodine electrolyte (for PbS) and a Pt counter electrode were used to construct the QDSSC architecture. The energy conversion efficiency of CdS QDSSC was 0.40% (short circuit current (J_{sc}) = 3.01 mAcm^{-2}, open circuit potential (V_{oc}) = 315.7 mV, fill factor (*FF*) = 0.424), and PbS QDSSC cell efficiency was 0.17% (J_{sc} = 0.515 mAcm^{-2}, V_{oc} = 559.2 mV, *FF* = 0.579) under the standard illumination conditions (AM 1.5G and 100 mW cm^{-2}) (see Figure S4 in Supporting Information). These efficiencies are smaller than similar QDSSC solar cell architechtures (FTO/mesoporous TiO_2/QD/Pt) prepared using the SILAR method (PbS:0.28%,[12] CdS:1.15%[11]) (see Table S1 in Supporting Information). It is noted that many factors to achieve the high solar cell efficiency were not optimized in this study. Those including the control of QD size, number of deposition cycles, TiO_2 architecture, selection of electrolytes, and surface passivation are being studied to improve the light harvesting ability of QDSSCs.

In conclusion, we successfully demonstrated that stoichiometric CuS, PbS, or CdS QDs can be deposited uniformly throughout the mesoporous TiO_2 film by coating the metal chalcogenide precursors dissolved in *l*-CO_2 followed by reacting the absorbed precursors with H_2S gas. The extremely low surface tension and the low viscosity of *l*-CO_2 resulted in a uniform concentration profile of the QDs throughout the mesoporous TiO_2 film with 15 μm thickness. The size of the QDs was 2.5−4.5 nm in diameter. Thus, it is possible to overcome one of the major barriers to achieving highly efficient QDSSCs, uniform deposition of QDs onto the meso/nanostructured oxide film, by using the *l*-CO_2 coating and the subsequent reaction technique.

Acknowledgment. This work was supported by the National Research Foundation of Korea Grant funded by the Korean Government (MEST) (NRF-2009-C1AAA001-2009-0092935). W. Jang and K.-P. Yoo thank the MOE for the studentship through BK21 program.

Supporting Information Available: Experimental procedures and photovolataic performance data of the QDSCs (PDF). This material is available free of charge via the Internet at http://pubs.acs.org.

(11) Lee, Y. L.; Chang, C. H. *J. Power Sources* **2008**, *185*, 584–588.
(12) Hyun, B.-R.; Zhong, Y.-W.; Bartnik, A. C.; Sun, L.; Abruña, H. D.; Wise, F. W.; Goodreau, J. D.; Matthews, J. R.; Leslie, T. M.; Borrelli, N. F. *ACS Nano* **2008**, *2*, 2206–2212.